Real-space renormalization-group study of fractal Ising models

B. Bonnier, Y. Leroyer, and C. Meyers

Laboratoire de Physique Théorique, Université de Bordeaux 1, rue du Solarium 33170 Gradignan, France

(Received 6 July 1987; revised manuscript received 29 September 1987)

Ising models on Sierpiński carpets are studied within a real-space renormalization technique. A specific method for decimating spin blocks of any size is proposed as an alternative to the bond-moving prescription, and its accuracy is checked on various examples. From an analysis of the critical couplings we estimate some of the finite-size effects of Monte Carlo simulations of fractals. The exponent ν, computed for a large variety of carpets, is found smaller than in the bond-moving approach but with the same behavior under variations of the fractal parameters. No universality criterion emerges except in the limit of vanishing lacunarity.

I. INTRODUCTION

Real-space renormalization-group (RSRG) techniques are widely used in determining the critical-point properties of lattice models, and in particular within the Migdal-Kadanoff (MK) approximation.[1] This method is simple in procedure but its numerical accuracy, in terms of critical temperatures and exponents, is often poor and various improvements of the initial MK bond-shifting prescription have been proposed.[2-4] These fail, however, when the rescaling factor is large, and the method may become inaccurate for systems such as fractals, where the RSRG technique necessarily involves the decimation of clusters of definite size. An illustrative example is provided by the Ising model on Sierpiński carpets,[5-8] which in the simplest case involves a rescaling factor 3. The MK-RSRG analysis can be confronted with numerical simulations[9,10] and, even in this simple case, an important discrepancy appears since ($K_c=0.32$, $\nu=4.46$) in Ref. 5, compared to ($K_c=0.47-0.49$, $\nu=1.04-1.12$) in Refs. 9 and 10, where K_c is the critical coupling and ν the inverse of the thermal exponent y_T. On the other hand, only a small number of such fractals have been numerically studied, since simulations become difficult and less reliable, due to finite-size and critical-slowing-down effects, when the lattice self-similarity factor increases. Critical properties are thus mainly available through the RSRG method, and the previous example indicates that a better approximation than the MK one is needed.

To undertake such a program, we construct in this work an effective coupling for the decimation of Ising spin cells of any size which can be applied to a RSRG analysis of Sierpiński carpets. We are thus led to consider as an initial system an Ising model with three ferromagnetic couplings K, K_I, and K_E on a lattice paved with clusters of inactive sites (gaps) involving two length parameters b and l. As shown in Fig. 1, these parameters are chosen in such a way that on a lattice of unit spacing, clusters of inactive spins of area l^2 are regularly nested inside cells of area b^2, the different couplings being needed to distinguish the internal bonds (K) from those on the boundaries (K_I and K_E). We then give the renormalized coupling Q resulting from the decimation of the Ising

spins inside the b^2 cells, for any value of the parameters. When the trivial remaining spins are integrated out, the final system is again an Ising one, and two cases are considered. When the initial system is a model with gaps, it is mapped onto a homogeneous one, and this allows us to obtain the phase diagrams of the gap models in the (K,K_I) plane. These diagrams, which may be derived in another more rigorous context,[11] are considered here as a consistency check of our effective coupling method. When the initial system is a Sierpiński carpet, the coupling Q is used to define a mapping between two successive iterations of the fractal, and the critical parameters K_c and ν are given by a fixed point analysis in the (K,K_I) plane.

This is done according to the following plan. In Sec. II, the method of construction of the effective couplings Q is developed and confronted to data. We show that functional relations between different Q allows us to consider only special couplings which involve the decimation of a minimal number of spins. These effective couplings are parametrized within a phenomenological cluster-decimation method which ensures that the critical parameters k_c and ν of the homogeneous Ising model have their exact value. As a result, phase diagrams of gap models are predicted, and we check that they agree up to $b=9$ with data we obtain through numerical simulations. Section III is devoted to the application of this effective coupling method to Ising models defined on Sierpiński carpets. It is used first to study the finite-size effects which appear when only a finite number of scales are implemented in the fractalization process. We then systematically compute the exponent ν in a flow analysis of the RSRG transforms of a whole family of carpets. Results are compared to the corresponding MK ones[5,7,8] and to the values found in an ϵ extrapolation at a noninteger dimension.[12] Finally we comment about the universality properties of these systems.

II. CONSTRUCTION OF THE EFFECTIVE COUPLINGS

We consider as an initial system the Ising model defined on a plane infinite lattice of unit spacing generat-
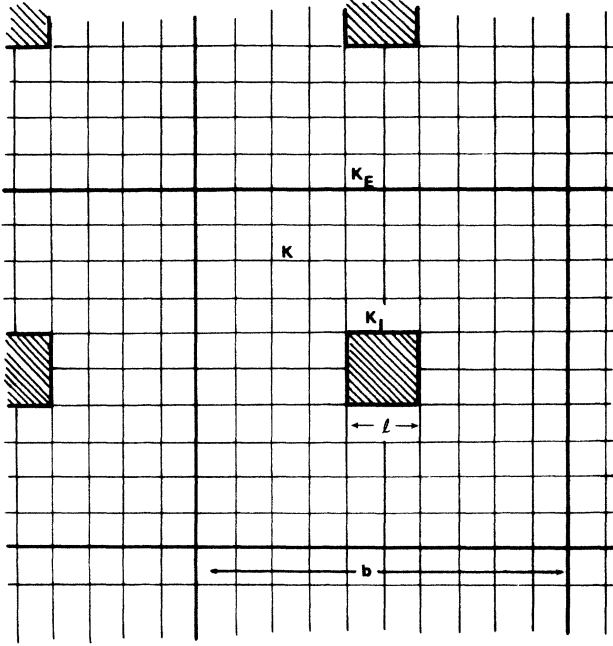
FIG. 1. A typical basic cell with $b=10$, $l=2$; the various couplings are exhibited: K_I along the gap boundary, K between internal spins, and K_E on the border of the cell.
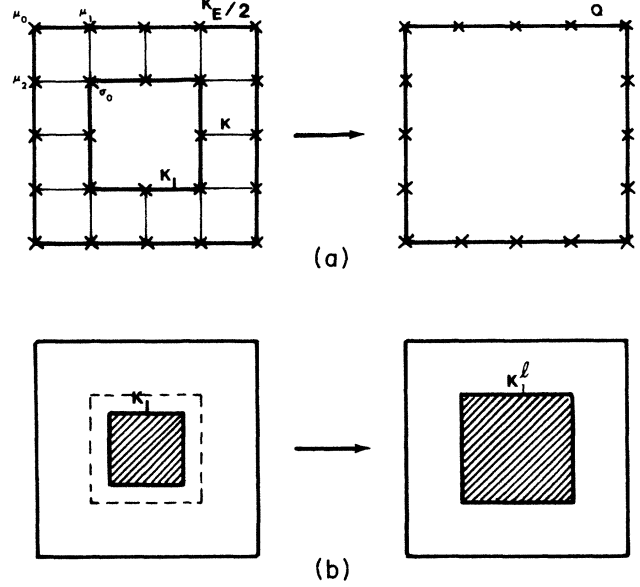

FIG. 2. (a) An illustration of the decimation scheme for a $(b,b-2)$ cell with $b=4$. (b) The first step of the recursive decimation Eq. (2.12). The $(l+2,l)$ cell delimited by the dotted line is decimated as in (a).

ed by periodically duplicating the Sierpiński carpet initiator shown in Fig. 1: from a square of side b is excised a central square of area l^2, and the spins are put at the corners of the remaining unit cells. Thus the integers b and l are both even or both odd with $l_0 \leq l \leq b-2$, where $l_0 = 0$ if b is even and $l_0 = 1$ if b is odd. The nearest-neighboring spins interact with ferromagnetic couplings K, K_I, and K_E according to the location of the bonds: K_E is the coupling between the spins $\{\mu_i\}$ on the external boundary of each pattern, the internal spins $\{\sigma_j\}$ being linked either through K or K_I if they are both on the internal boundary of the basic pattern.

The RSRG transforms we perform are made up of the usual steps. First, the cells are decimated of all their internal spins $\{\sigma_i\}$, with the convention that the common links, which carry the coupling K_E, are symmetrically assigned to each cell. One then assumes that the renormalization (per cell) of the coupling between the remaining spins $\{\mu_i\}$ is of the form [illustrated in Fig. (2a) for $l=b-2$]

$$K_E/2 \rightarrow Q(b,l;K,K_I,K_E) .$$ (2.1)

Then one integrates out the trivial degrees of freedom associated with the $\{\mu_i\}$ spins which have only two neighbors. The resulting system is again an Ising one, with a lattice spacing b and a coupling Q' between neighbors, given by

$$\tanh Q' = \tanh^b[2Q(b,l;K,K_I,K_E)] ,$$ (2.2)

where the factor 2 in Eq. (2.2) comes from the added contributions (2.1) of two adjacent cells. When $l=l_0$, $K_E = K_I = K$, the transform $K \rightarrow Q'(K)$ is a RSRG of the homogeneous Ising model under a rescaling factor b and

its fixed point k_c must satisfy the conditions

$$\tanh Q'(k_c) = \tanh k_c = \sqrt{2} - 1 ,$$ (2.3)

$$y_T = \frac{1}{\nu} = \frac{1}{\ln b} \ln \left[\left| \frac{dQ'}{dK} \right|_{K=k_c} \right] = 1 .$$ (2.4)

In the general case $l > l_0$, Eq. (2.2) defines a mapping between a gap model and a homogeneous one, in such a way that the critical lines $C(b,l;K,K_I)$ are the images of the fixed point (2.3) and are thus given by

$$Q(b,l;K,K_I,K) = q_b = \frac{1}{2}\tanh^{-1}[(\sqrt{2}-1)^{1/b}] .$$ (2.5)

In order to improve the bond-moving prescription which reads[5]

$$\tanh^b[2Q(b,l;K_I,K_E)] = \tanh^{b-l}[K_E + (b-1)K]$$

$$\times \tanh^l[K_E + 2K_I$$

$$+ (b-l-2)K] ,$$

(2.6)

we proceed in two steps: First we construct for any b the special couplings $Q(b,b-2;K,K_I,K_E)$ involving minimal decimations, and then show they give the remaining ones $Q(b,l;K,K_I,K_E)$ for any l with $l_0 \leq l \leq b-2$.

As for the minimal decimations shown on Fig. 2(a) we choose the representation

$$\tanh^b[2Q(b,b-2;K,K_I,K_E)]$$

$$= \tanh^{b-2}(K_E + 2K_I)\tanh^2(2Q_1)$$ (2.7)

which involves the prescription (2.6) for moving a single bond and an effective coupling Q_1 for the corner spin decimation, which is conveniently parametrized within a

cluster-decimation method.[4] We thus associate to the cluster $\{\sigma_0\mu_0\mu_1\mu_2\}$—see Fig. 2(a)—the functions

$$E_1 = \operatorname*{Tr}_{\sigma_0=\pm1} \exp\left[\rho\frac{K_E}{2}(\mu_0\mu_1+\mu_0\mu_2)+\rho K(\sigma_0\mu_1+\sigma_0\mu_2)\right],$$

(2.8)

$$E_2 = \exp[Q_1(\mu_0\mu_1+\mu_0\mu_2)]$$

(2.9)

before and after decimation, respectively, and determine Q_1 by equating their average on aligned configurations of the $\{\mu_0\mu_1\mu_2\}$ spins. This gives

$$\tanh Q_1 = (1+\tau)\left[\frac{1+t^2}{1+t^2\tau^2}\right]^{1/2} - 1,$$

(2.10)

where $\tau=\tanh(\rho K_E/2)$ and $t=\tanh(\rho K)$. The factor ρ, $\rho>1$, which in Eq. (2.8) enhances the couplings, is usually interpreted as the effect of the whole lattice on the 2×2 clusters and will be fixed later on.

We now sketch how the special couplings $Q(n,n-2;K,K_I,K_E)$, $2\le n\le B$ determine the remaining ones $Q(b,l;K,K_I,K_E)$ where $2\le b\le B$, $l_0\le l\le b-2$. Consider, as in Fig. 2(b), the $(l+2,l)$ central cell in the basic (b,l) block. After decimation of this cell we get a gap of size $(l+2,l+2)$ of which the boundary carries a new coupling K_1 given, according to our prescriptions, by

$$K_1 = \frac{K}{2}+Q(l+2,l;K,K_I,K).$$

(2.11)

Repeating this procedure by increasing the size of the central decimated cell up to its maximum value $b-2$, we get the recursion relation

$$K_n = \frac{K}{2}+Q(l+2n,l+2n-2;K,K_{n-1},K)$$

(2.12)

with $K_0=K_I$. The last decimation $n=N=(b-l-2)/2$ gives the wanted expression

$$Q(b,l;K,K_I,K_E)=Q(b,b-2;K,K_N,K_E).$$

(2.13)

An interesting consequence of the previous functional relations is that the fixed point constraints, which in Eqs. (2.3) and (2.4) apply for any b for $l=l_0$ only, propagate to the whole set $l>l_0$. In particular for the special couplings where $l=b-2$, they read

$$Q(b,b-2;k_c,k_b,k_c)=q_b,$$

(2.14)

$$\delta Q(b,b-2;k_c,k_b,k_c)=\tilde q_b,$$

(2.15)

where δ is the differential operator defined as

$$\delta F(k_c,k_b)=\left[\frac{\partial}{\partial K}+\tilde k_b\frac{\partial}{\partial K_I}\right]F(K,K_I)\Big|_{K=k_c,K_I=k_b},$$

(2.16)

and in which

$$k_b=\frac{k_c}{2}+q_{b-2}, \quad \tilde q_b=\frac{1}{2\sinh(2k_c/b)},$$

$$\tilde k_b=\tfrac{1}{2}+\tilde q_{b-2}$$

(2.17)

These relations, easily derived by induction from Eqs. (2.3) and (2.4), must constrain the parameter ρ we have left unspecified, once the representations (2.7) and (2.10) for $Q(b,b-2;K,K_I,K_E)$ are inserted in Eqs. (2.14) and (2.15). However we first observe that Eq. (2.14) predicts independently of any parametrization that the point $(K=k_c,\ K_I=k_b)$ lies on the critical line $C(b,b-2;\ K,K_I)$, which can be measured. We have checked, using Monte Carlo simulations, that this is indeed the case, as shown, for example, in Fig. 3. As for the parametrization of ρ, we observe that in the asymptotic regime $b=\infty$ the constraints (2.14) and (2.15) lead to a step function behavior

$$\rho\sim1.2425, \quad \delta\rho\sim1.2313b-2.7591$$

(2.18)

which can be well reproduced by a variable like $\tanh^{b-2}(2k_cK_I/K)$ and we then choose, in accordance with the data depicted below, the following forms:

$$b=2, \quad \rho=\text{const}=1.1395 \quad (\text{then } \nu=1.04),$$

(2.19)

$$b=3, \quad \rho=1+\lambda\tanh^\mu(K+K_I),$$

(2.20)

$$b=4,$$

(2.21)

$$\rho=1+\lambda\tanh(2K)\tanh\left[2k_c\frac{K_I}{K}\right]\tanh^\mu\left[K+\frac{k_c}{k_b}K_I\right],$$

$$b\ge5,$$

(2.22)

$$\rho=1+\lambda\tanh^{b-2}\left[2k_c\frac{K_I}{K}\right]\tanh^\mu\left[K+\frac{k_c}{k_b}K_I\right],$$

where (λ,μ) are adjusted as to fulfill the constraints (2.14) and (2.15).

In order to compare some critical lines $C(b,l;K,K_I)$ given by our effective couplings with data, we have performed Monte Carlo simulations of the Ising model with gaps for the values $b=3,4,5,6,7,9$ and l in the range $l_0\le l\le b-2$. This study has been performed on a Digital Equipment Corporation VAX11/750 computer and requires about 500 h of CPU time. For a given choice of
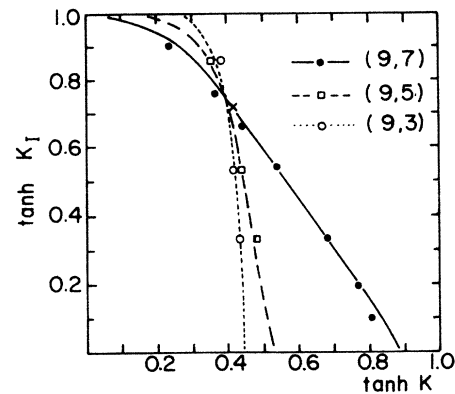

FIG. 3. The critical lines for $b=9$ and $l=3,5,7$ Ising gap model together with the Monte Carlo data of these systems. The error bars are smaller than the size of the dot. The cross corresponds to the point $K=k_c$, $K_I=k_b$.

the b and l values, the system which is numerically simulated is made up of a sufficient number of basic cells as to correctly reproduce the thermodynamical regime, whose approach is controlled by increasing the size of the system. Choosing $b = 9$ as a typical example, the simulations use 4–9 replicas, and we estimate the errors to be smaller than the size of the data points shown on Fig. 3. The agreement of the various lines $C(9,l;K,K_I)$ with the data is good, and this is the case for all the simulated cases. As an alternative to the bond-moving approximation we then apply this effective coupling method to fractal models in the next section.

III. THE FRACTAL ISING MODEL

We take as lattices a family of Sierpiński carpets defined as follows:[6] Let (p,b,l) be three integers such that $p > 0$ and $1 \leq l \leq b - 2$. The initiator is obtained by dividing a square into p^2 subsquares each one being itself divided into b^2 elementary cells and then erasing l^2 of those cells in the center of each of the p^2 intermediate subsquares. To construct the fractal, this procedure is indefinitely applied to the elementary cells. The number of elementary cells in the initiator is $(pb)^2 - (pl)^2$, and therefore the fractal dimension of this system is $D = \ln[p^2(b^2 - l^2)]/\ln pb$. The Ising model is defined on that lattice in the same way as in Sec. II.

The RSRG transforms of such models involve a rescaling factor pb leaving the lattice invariant while the couplings (K,K_I) evolve into (K',K_I'), which are easily derived as follows from the method of Sec. II. We have to map blocks of size $(pb)^2$, which can be empty or initiator like, onto unit cells. In the later case we first decimate all the intermediate b^2 cells to obtain p^2 empty cells of size b^2, with a boundary coupling K_1' given by

$$\tanh K_1' = \tanh^b 2Q(b,l;K,K_I,K_E) \ , \tag{3.1}$$

where K_E, which is either K or K_I according to the location of the cell, is fixed at its mean value in the fractal. Going then to a unit cell we end up with the renormalized coupling K'.

$$\tanh K' = \tanh^p 2Q(p,p_0;K_1',K_1',K_1') \ , \tag{3.2}$$

where p_0 is 0 or 1 if p is even or odd, respectively. One can thus assume that decimating blocks of size $(pb)^2$ from their internal spins renormalizes the coupling between the boundary spins into K_2', given by

$$\tanh^{pb} 2K_2' = \tanh K' \ . \tag{3.3}$$

Considering now an empty block of size $(pb)^2$ and decimating its neighboring $(pb)^2$ blocks according to the rule (3.3) gives the renormalized coupling K_I' through

$$\tanh K_I' = \tanh^{pb}(K_I + K_2') \tag{3.4}$$

We perform a standard analysis of the previous mapping Eqs. (3.1)–(3.4) to obtain the critical coupling K_c (the point where $K = K_I$ on the critical flowline) and the thermal exponent (by linearization around the nontrivial fixed point). In addition, we study the way K_c is reached when the number n of fractal iterations increases to

infinity. This may be relevant for existing or future Monte Carlo simulations as it reveals a new kind of finite-size effects ("finite-fractalization effects").

We thus consider lattices which are an infinite replication of a basic pattern being itself an iterate, at stage n, of some carpet ($n = 1$ corresponds to the initiator, $n = \infty$ to the fractal). Such a model is mapped onto an homogeneous one, which gives its phase diagram in the (K,K_I) plane, and we focus on the critical coupling Q_n, i.e., the point on this line where $K = K_I$. As n increases, the sequence $\{Q_n\}$ converges to K_c, and more generally the nth phase diagram converges towards the critical-flow line of the RSRG mapping. The interest of the sequence $\{Q_n\}$ is that it is close to the corresponding one $\{Q_n'\}$ which can be observed in a Monte Carlo analysis of the nth fractal iteration. In fact $Q_n' \leq Q_n$ and $Q_n' \cong Q_n$ only when "usual" finite-size effects are removed, for example, by duplicating the basic pattern in the numerical analysis: Up to 16 patterns have been used in a simulation of the ($p = 1$, $b = 5$, $l = 3$) system we have performed and which confirms our predictions for Q_2 and Q_3. On this example, shown in Fig. 4, we observe that the fractal limit is slowly reached ($Q_1 = 0.52$, $Q_2 = 0.60$, $Q_3 = 0.62$, $K_c = 0.64$). This effect is found to increase as the fractal dimension D decreases and suggests that in general 4 to 5 iterations are necessary in a numerical simulation to obtain a reliable evaluation of K_c. Therefore, this effect can spoil the determination of the critical exponents which crucially depend on the value of K_c. Indeed, in a previous numerical analysis using two fractal iterations only,[10] we have estimated K_c to be at most 0.61 and 0.72 for the ($p = 1$, $b = 5$, $l = 3$) and ($p = 1$, $b = 7$, $l = 5$) systems, respectively, instead of $K_c = 0.64$ and $K_c = 0.79$ in the present analysis. As the exponents appear to increase with the assumed value for K_c, we also underestimated ν in that work ($\nu = 1.45$ and 1.87 instead of 1.6 and 2). On the other hand, for a system like ($p = 1$, $b = 3$, $l = 1$) which has a dimension $D = 1.89$, this effect appears to be negligible and in fact the numerical results[9,10] are in
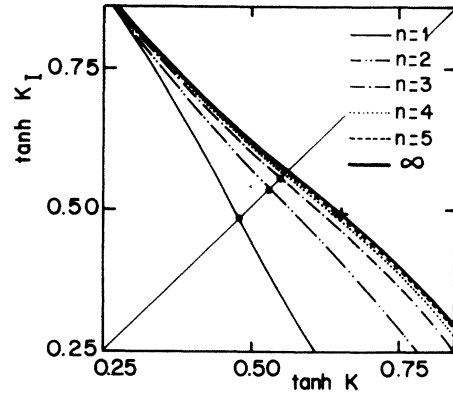

FIG. 4. The critical lines for the ($p = 1$, $b = 5$, $l = 3$) system at its first five iterates. The thick solid line is the critical-flow line corresponding to the infinite fractal iterations limit. The cross on this line is the nontrivial fixed point. The data points are from a Monte Carlo simulation.

TABLE I. Some of the Sierpiński carpets that we have investigated, characterized by the value of their parameters p,b,l. For each case we give the fractal dimension D, the dynamic dimension d_S, the lacunarity L, and the value of the exponent v resulting from the MK method and from our method.

p	b	l	D	d_S	L	v_{MK}	v
1	3	1	1.893	1.909	0.170	4.46	1.12
1	4	2	1.862	1.825	0.220	2.67	1.29
1	5	3	1.723	1.721	0.262	2.60	1.53
1	5	1	1.975	1.983	0.083	1.47	1.08
1	7	5	1.633	1.676	0.307	2.92	1.93
1	7	3	1.896	1.887	0.186	1.91	1.31
1	7	1	1.989	1.994	0.050	1.44	1.09
1	9	7	1.577	1.656	0.330	3.24	2.29
1	9	5	1.832	1.852	0.251	2.27	1.49
2	3	1	1.934	1.958	0.053	1.73	1.08
2	4	2	1.862	1.825	0.062	2.33	1.35
2	5	3	1.806	1.770	0.106	2.51	1.51
2	7	5	1.730	1.721	0.152	2.73	1.70
3	5	3	1.835	1.784	0.056	2.17	1.48
3	5	1	1.985	1.994	0.016	1.42	1.09
3	7	5	1.766	1.734	0.086	2.28	1.64
3	7	3	1.933	1.904	0.042	1.64	1.26
5	5	3	1.861	1.795	0.033	2.03	1.28
5	7	5	1.799	1.744	0.046	2.08	1.37
5	7	3	1.943	1.907	0.023	1.60	1.19

agreement with the present RSRG analysis ($K_c = 0.485$, $v = 1.12$). This is simply an illustration that finite-fractalization effects are driven by the exponent v which grows as D decreases. Consequently, when D gets significantly lower than 2, as only the first few iterates are numerically accessible, it seems very difficult to perform a reliable extrapolation of the critical parameters.

In the next part of our analysis of fractals, we have systematically determined the critical exponent v for a wide family of Sierpiński carpets whose parameters lie in the range (chosen to remain within the domain of validity of our method following paragraph 2):
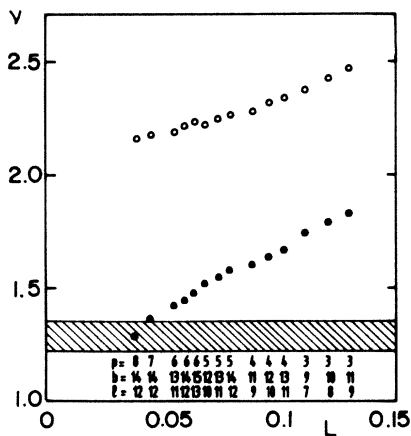

FIG. 5. The exponent v vs the lacunarity at fixed $D = 1.70 \pm 0.02$. For each lattice, whose (p,b,l) parameters are mentioned at the bottom of the plot, we show our results (solid points) and the MK ones (open points). The dashed area corresponds to the ϵ expansion calculation of Ref. 12 for $d = 1.70 \pm 0.02$.

$$1 \leq p \leq 8, \quad 3 \leq b \leq 14, \quad l_0 \leq l \leq b - 2 . \quad (3.5)$$

A sample of our results is presented in Table I, listed according to the parameters (p,b,l). For each case we have computed some of the general geometrical parameters such that the fractal dimension D and the lacunarity L. Actually, fractal lattices being not translationally invariant, one expects the critical parameters to depend on the lacunarity, which is defined as the fluctuation about its mean value of the mass of a small random piece of fractal. Among the various definitions of this quantity[7,8,13] we adopt that of Ref. 8 [more precisely $L_3(l,b)$ in the notation of Ref. 8]. As (p,b,l) vary in the range defined by the inequalities (3.5), D and L are restricted to

$$1.5 \lesssim D \lesssim 2, \quad 0.01 \lesssim L \lesssim 0.35 . \quad (3.6)$$

In addition to Table I, where only carpets with small initiator are collected, we present in Fig. 5 the exponent v for some other lattices involving larger values of (p,b,l) (quoted at the bottom of the plot) selected according to their fractal dimension fixed at $D = 1.70 \pm 0.02$ and varying lacunarity. From the whole data it appears that v is more a smooth function of the fractal parameters D and L than of (p,b,l). The values of v obtained from the bond-moving technique are shown in Table I and Fig. 5. They appear to be appreciably higher than ours but follow the same behavior, namely at fixed D and $L \leq 0.1$, v decreases with L.

To conclude we comment about the conjecture that fractals may interpolate hypercubic lattices in noninteger dimension. Our results confirm that the critical exponent strongly depends on the lacunarity in addition to the fractal dimension which thus cannot play the role of the extrapolated dimension d. A dynamical dimension d_S, defined as the average number of bond per site, has been proposed,[5,10,14] and we have quoted its value for the Sierpiński carpets of Table I. Analyzing the whole data with d_S in place of D does not qualitatively change our conclusions. For instance whether d_S or D is considered we observe that our v values are almost always higher than the ones predicted by the ϵ expansion calculations at noninteger dimension d,[12] and only for small lacunarity do the two results get close to each other. The MK results present the same general trend but with appreciably larger values of v even in the low-lacunarity region. However, following the suggestion of Ref. 6 the Φ_d^4 universality class may be recovered in the limit of zero lacunarity. The behavior of v as a function of L displayed in Fig. 5 support this conjecture as an extrapolation of the data to zero lacunarity is roughly in agreement with the ϵ expansion result. Nevertheless, the low-lacunarity region, corresponding to lattices with very large initiator, is not easily accessible from a computational point of view, and this obviously weakens the interest raised by these kind of fractals.

[1]A. A. Migdal, Zh. Eksp. Teor. Fiz. **69**, 1457 (1975); **69**, 810 (1975) [Sov. Phys.—JETP **42**, 743 (1975); **42**, 413 (1975)]; L. P. Kadanoff, Ann. Phys. (NY) **100**, 359 (1976).

[2]T. W. Burkhardt, in *Real-Space Renormalization,* edited by T. W. Burkhardt and J. M. M. Van Leewen (Springer-Verlag, Berlin, 1982).

[3]G. Martinelli and G. Parisi, Nucl. Phys. **B180**, 201 (1981); J. S. Walker, Phys. Rev. B **26**, 3792 (1982); R. E. Goldstein and J. S. Walker, J. Phys. A **18**, 1275 (1985).

[4]H. H. Chen, Felix Lee, and H. C. Tseng, Phys. Rev. B **34**, 6448 (1986).

[5]Y. Gefen, B. B. Mandelbrot, and A. Aharony, Phys. Rev. Lett. **45**, 855 (1980); Y. Gefen, A. Aharony, and B. B. Mandelbrot, J. Phys. A **17**, 1277 (1984).

[6]Y. Gefen, Y. Meir, B. B. Mandelbrot, and A. Aharony, Phys. Rev. Lett. **50**, 145 (1983).

[7]R. Riera and C. M. Chaves, Z. Phys. B **62**, 387 (1985); B. Lin, J. Phys. A **20**, L163 (1987); P. Y. Lai and Y. Y. Goldschmidt, *ibid.* **20**, 2159 (1987).

[8]Y. K. Wu and B. Hu, Phys. Rev. A **35**, 1404 (1987).

[9]J. C. Angles d'Auriac and R. Rammal, J. Phys. A **19**, L655 (1986).

[10]B. Bonnier, Y. Leroyer, and C. Meyers, J. Phys. (Paris) **48**, 553 (1987).

[11]J. J. M. Rijpkema and H. J. F. Knops, Physica **122A**, 489 (1983).

[12]J. C. Le Guillou and J. Zinn-Justin, J. Phys. (Paris) **48**, 19 (1987).

[13]B. Lin and Z. R. Yang, J. Phys. A **19**, L49 (1986).

[14]G. Bhanot, D. Duke, and R. Salvador, Phys. Lett. **165B**, 355 (1985).